Dendrochronologia 31 (2013) 297–310

Contents lists available at ScienceDirect

Dendrochronologia

journal homepage: www.elsevier.com/locate/dendro

Exploring teleconnections between the summer NAO (SNAO) and climate in East Asia over the last four centuries – A tree-ring perspective

Hans W. Linderholm[a,*], Andrea Seim[a], Tinghai Ou[a], Jee-Hoon Jeong[a,f], Yu Liu[a,b], Xiaochun Wang[c], Guang Bao[d], Chris Folland[a,e]

[a] Regional Climate Group, Department of Earth Sciences, University of Gothenburg, Gothenburg, Sweden
[b] State Key Laboratory of Loess and Quaternary Geology, Institute of Earth Environment, Chinese Academy of Sciences, Xi'an, China
[c] Center for Ecological Research, Northeast Forestry University, Harbin, Heilongjiang, China
[d] Key Laboratory of Disaster Monitoring and Mechanism Simulating of Shaanxi Province, Baoji University of Arts and Sciences, Shaanxi, China
[e] Met Office Hadley Centre for Climate Change, Exeter, UK
[f] Faculty of Earth Systems & Environmental Sciences, Chonnam National University, Gwangju, Korea

ARTICLE INFO

Article history:
Received 19 March 2012
Accepted 19 August 2012

Keywords:
East Asian climate
Summer NAO
Teleconnection
Tree-ring width network

ABSTRACT

The summer North Atlantic Oscillation (SNAO), derived from the first EOF of mean sea level pressure over the extratropical North Atlantic in July and August, has a close association with climate variability over the North Atlantic region, and beyond, on both short and long time scales. Recent findings suggested a teleconnection, through the SNAO, linking climate variability over Northern Europe with that of East Asia in the latter part of the twentieth century. Here we investigate the temporal stability of that teleconnection for the last four centuries using 4261 tree-ring width series from 106 sites and, additionally, ten climate reconstructions from East Asia. Our results showed a great potential in using tree-ring width (TRW) data to extend analyses of the SNAO influence on East Asian climate beyond the instrumental period, but preferably with a denser network. The strongest SNAO-TRW associations were found in central East Asia (in and around Mongolia) and on the eastern edge of the Tibetan Plateau. In addition, the analysis showed that the association between the SNAO and East Asian climate over the last 400 years has been variable, both among regions and at specific sites. Moreover, a clear difference in the SNAO-TRW associations was found on two examined time scales, being stronger on longer timescales. Our results indicate that TRW data can be a useful tool to explore the remote influence of the SNAO on East Asian climate in the past.
© 2013 Elsevier GmbH. All rights reserved.

Introduction

The summer NAO (SNAO)

The North Atlantic Oscillation (NAO) is one of the leading atmospheric modes associated with climate variability in the North Atlantic region (Hurrell and van Loon, 1997). For obvious reasons, the most pronounced influences on climate can be found in Europe and eastern North America, where variability in temperature, precipitation, cloudiness etc., can be linked to the NAO (Hurrell et al., 2003). However, significant association have also been found between the NAO and climate outside this region (see e.g. Fig. 1 in Visbeck et al., 2001). While the NAO pattern is most prominent during winter, leading atmospheric circulation patterns similar to the winter NAO are also found in the other seasons (Hurrell and van Loon, 1997), although the pattern shifts in size and geographical location over the year (e.g. Barnston and Livezey, 1987; Hurrell et al., 2003). Applying an eigenvector (EOF) analysis to summer (July–August, JA) mean sea level pressure (MSLP) data over the North Atlantic region, Hurrell and Folland (2002) obtained a dipole pattern similar to the winter NAO, where its southern node was centred over UK and Scandinavia rather than the Azores – Spain region seen in winter. It was noted that the summer NAO (hereafter SNAO) time series showed large interannual to decadal variability, where the transition from a predominantly negative SNAO phase to a positive one in the 1960s stood out. A more thorough investigation of the SNAO was presented by Folland et al. (2009), where a strong link with JA climate, predominantly over Northern Europe was shown, indicating a strong influence of the atmospheric circulation on high-latitude climate also in summer. During positive SNAO years, the southern node has anomalously high pressure and the northern node over the Arctic has anomalously low pressure. This is the same convention as used for the winter NAO, though the southern node moves north eastward in summer compared to the

* Corresponding author. Tel.: +46(0)217862887; fax: +46(0)317861986.
E-mail address: hans.linderholm@gvc.gu.se (H.W. Linderholm).

1125-7865/$ – see front matter © 2013 Elsevier GmbH. All rights reserved.
http://dx.doi.org/10.1016/j.dendro.2012.08.004

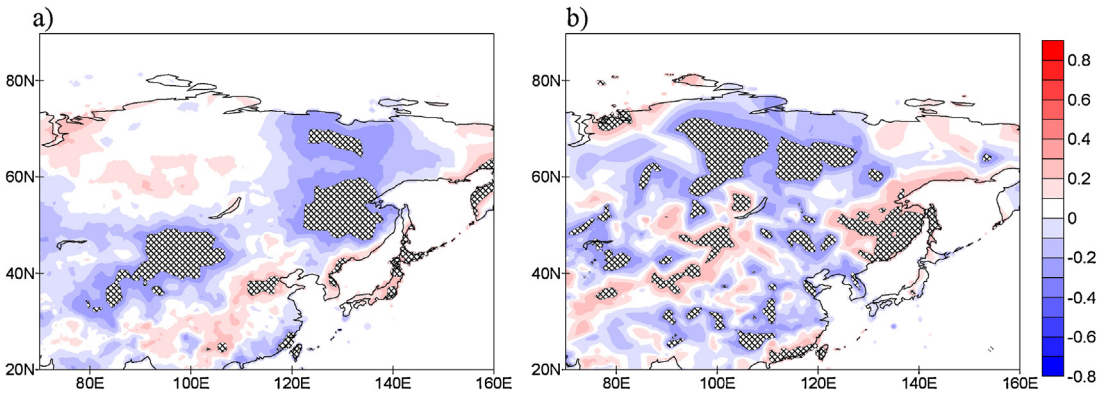

Fig. 1. Spatial correlation between SNAO (Folland et al., 2009) and (a) mean JA temperature and (b) total JA precipitation (CRU TS 2.1, Mitchell and Jones, 2005), for the 1951–1990 period. Correlations significant at the 0.05 level are indicated by crosses, and all data was 9 point high-pass filtered.

winter NAO and the Arctic node is smaller in area. In the positive SNAO phase, conditions are warmer and drier, with less clouds than normal, over Northern Europe as far east as most of Scandinavia. Although the anomalous JA MSLP pattern over southern Europe is weak, it tends to be opposite to that over Northern Europe giving the hint of a tripole structure. However, the surface climate anomalies are more distinctly the opposite of those over Northern Europe, especially for precipitation (Folland et al., 2009; Linderholm et al., 2009). Additionally, strong correlations with temperature and precipitation can be found elsewhere in the world, especially over North America and the North African monsoon region, indicating that the SNAO is linked to climate variability more widely (see Figs. 4–6a in Folland et al., 2009).

SNAO and summer climate in East Asia

Summer climate in East Asia is strongly affected by the East Asian monsoon circulation induced by the large-scale land-sea thermal contrast (An, 2000; Ding, 2004; Cook et al., 2010), and thus closely associated with tropical and subtropical sea-surface temperatures associated with the El-Niño Southern Oscillation (ENSO) and land surface conditions like winter and spring snow and soil moisture in the Eurasian continent (e.g. Wang B., 2006a). Moreover, several studies have investigated the delayed remote influences from the winter and spring NAO (and Arctic Oscillation, AO) on climate variability in the region, especially in the western and northern areas which are influenced by the westerly winds (e.g. Gong and Ho, 2003; Sung et al., 2006; Xin et al., 2006; Li et al., 2008; Hong et al., 2008; Gu et al., 2009). A few studies have found associations between climate and the SNAO, but a confusing factor is that the definition of summer and the SNAO has varied (e.g. Liu and Yin, 2001; Wang et al., 2003; Sun et al., 2008). In a study focusing on the association between the SNAO (as defined by Folland et al., 2009) and summer climate in East Asia, utilizing observations and reanalyzes data for the last 50 years, Linderholm et al. (2011) showed that some major patterns of summer climate over China, including the East Asian Summer Monsoon, were associated with the interannual variation of the SNAO, suggesting that a teleconnection between the North Atlantic region and East Asia previously found in winter (see Sung et al., 2010), could also be observed in JA. The spatial correlation pattern of the SNAO versus temperature and precipitation in East Asia described by Linderholm et al. (2011) is shown in Fig. 1. These teleconnections were explained by Fig. 2 of Linderholm et al. (2011), and relate to changes in the position of the North Atlantic and downstream storm tracks associated with the two phases of the SNAO. In negative SNAO years, the storm tracks take a more southerly path over the northeast Atlantic and northwestern Europe towards southern Asia, with reduced storm track activity over Mongolia and North East China. During positive SNAO years, the storm-tracks takes a more northerly path across the northeast Atlantic into northern Russia and is re-strengthened over northeast China and towards Kamchatka. In southeast China, there is much less influence of the SNAO but the negative phase of the SNAO may slightly reduce storm track activity there. So as far as relationships with storm track activity and rainfall are concerned, the biggest effects of the SNAO on paleoclimate data in East Asia might be expected in Mongolia and northeast China if these effects are stable in time.

This paper presents the initial results of a study where we extend the work done by Linderholm et al. (2011) well before the period they studied, i.e. 1951-2002. This was a period strongly influenced by recent surface warming. So the question arises: are these results representative of persistent teleconnections over past centuries, or a just feature of the last few climatically warmer decades? Due to the general lack of instrumental observations prior to the 1950s in large parts of East Asia, proxy data is needed to investigate this. Here we utilized a network of available tree-ring width (TRW) data, as well as a set of climate reconstructions, from East Asia. The aim of this preliminary study was to: (1) assess the possibility of using an East Asian TRW network to assess the nature of the SNAO teleconnection prior to the mid-twentieth century; (2) investigate the spatiotemporal stability of the teleconnection over the last 400 years; and (3) examine the nature of the teleconnection on (a) interannual time scales and (b) decadal and longer time scales.

Data

Observational data

As in Folland et al. (2009), the SNAO index is represented by the principal components time-series of the leading EOF of daily MSLP anomalies from the EMULATE data set (Ansell et al., 2006) over extratropical European–North Atlantic sector (25–70° N, 70° W–50° E) for July and August 1881–2003 (Fig. 2). The leading EOF explains about 18% of the daily variance and 28% of the JA mean variance over the domain. It should be noted that the EOF analyses mainly reproduces the southern part of the full SNAO pattern. Thus, when the southern node has higher (lower) than average pressure, the SNAO index is in a positive (negative) phase.

To represent instrumental temperature and precipitation in East Asia (in this study 20–80° N, 70–160° E), we used two gridded

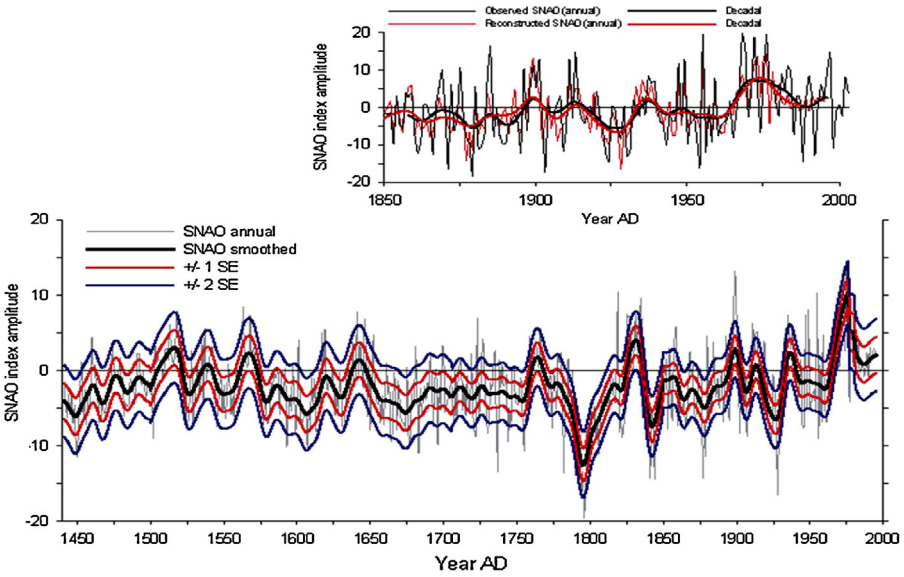

Fig. 2. Upper figure shows the reconstructed (Linderholm et al., 2008) versus the observed SNAO 1850–1995. Lower figure shows the full reconstruction, with 1 and 2 standard errors (SE). Note that the SE is based on the decadal values. Thick lines represent smoothed (Gaussian filtered, $\sigma = 3$) values, highlighting variability on timescales >10 years.

data sets. Temperature and precipitation were represented by the 0.5° × 0.5° resolution observed global land temperature dataset from the Climate Research Unit; CRU TS 2.1 (Mitchell and Jones, 2005, data available at http://www.cru.uea.ac.uk/). Judging from previous successful comparisons between the CRU TS 2.1 and several observational climate datasets in China (Wen et al., 2006), this gridded data is expected to represent our study region quite well.

In large parts of our study area, the influence of ENSO on East Asian climate should be more pronounced than that of the SNAO. Thus, to distinguish between the influences of these two indices, we made additional analyses using an ENSO index (see Methods Section). In the instrumental period, ENSO was represented by the HadSST1 (Rayner et al., 2003) Niño 3 Index (data downloaded from Climate Explorer, http://climexp.knmi.nl/). This index was created by averaging SST anomalies across the 5° N–5° S, 90–150° W region in the central Pacific (Trenberth, 1997), and we used the June through August (JJA) Niño 3 index in the twentieth-century analysis.

Reconstructed data

It was shown by Folland et al. (2009) that tree-ring data from the southern node region could be used to quite successfully reconstruct the SNAO back to the early 1700s. An extended version of the reconstruction, based on the work of Linderholm et al. (2008), going back to 1441 was used in the analyses of drought in Europe and central Africa by Linderholm et al. (2009). The extended reconstruction utilized the information that the SNAO shows significant correlations with temperature and precipitation outside Europe as well (see above). Consequently, tree-ring data from all around the North Atlantic sector were used as SNAO predictors. Thus, this reconstruction was expected to contain a spatially larger signal that the previous, shorter one. The SNAO reconstruction explained up to 46% of the variance in the instrumental SNAO back to 1850. The reconstruction is shown in Fig. 2. For more details, see Linderholm et al. (2008, 2009).

To assess the relative influence of the SNAO and ENSO over the last four centuries, we utilized a tree-ring based reconstruction of ENSO by Cook (2000, data obtained at http://www.ncdc.noaa.gov/paleo/data.html). Unfortunately, no reconstructions of summer ENSO are available; the one used here represents the Niño 3 index of ENSO variability from December through February (DJF), and covers the period 1408–1978. Since ENSO on average changes rapidly after DJF, so that by April–May the correlation with DJF falls quickly (the so called spring predictability barrier, e.g. Walker, 1995), DJF Niño 3 cannot be used as a proxy for the following JJA conditions. However, the correlation between observed JJA (correlation coefficient between JJA and JA Niño 3 index is 0.99, 1870–2010) and the *following* DJF indices is high ($r = 0.80$, 1870–2010), and the agreement persists on low frequencies, so the assumption here is that taken the above relationship into consideration, the reconstruction can be regarded as a useful proxy for summer conditions. More details about the reconstruction can be found in D'Arrigo et al. (2005).

East Asian tree-ring data

To explore the link between the SNAO and climate in East Asia in the pre-instrumental period, we used a network of TRW chronologies collected from 106 sites (including 4261 TRW series) across the 27–66° N and 81–145° E region, focusing on the regions where significant correlation patterns were found in Linderholm et al. (2011). The main part (98 sites) was taken from the International Tree-Ring Data Bank (ITRDB, http://www.ncdc.noaa.gov/paleo/treering.html), while the remaining eight datasets were contributed by the co-authors (Table 1). The sites were located in an elevation span from 50 to 4260 m a.s.l., where the TRW data contains a wide range of possible climatic information. To enhance the density of the proxy network, we also included a set of reconstructions (Table 2): four of temperature (Davi et al., 2001; Tan et al., 2003; Bräuning and Mantwill, 2004; Yi et al., 2012), five of precipitation (Hughes et al., 1994; Yi et al., 2010, 2012) and one of stream flow (Davi et al., 2006), all obtained from http://www.ncdc.noaa.gov/paleo/recons.html. It should be noted that the reconstructions are not exclusively based on tree-ring data, but do also contain other proxies.

Table 1
Site chronology characteristics are shown including site code (italics indicate code for the standardized chronologies from the ITRDB), geographical position (latitude and longitude in degrees), elevation (m a.s.l.), genera, number of series per site, start and end year and total length of the chronologies (>5 series). MSL represent the mean segment length, Rbar the inter-series correlation and L-1 the autocorrelation with the previous year of tree growth. Contributor and reference (bold) is provided in the last column.

Country	Site code	Site Location	Lat (°N)	Long (°E)	Elev (m a.s.l.)	Genus	Series (N)	Start year (>5 N)	End year	Length (>5 N)	MSL	Rbar	Investigator
China	*BRT02*	Boritu02	47.83	119.48	894-915	*Pinus* sp.	35	1886	1989	104	–	0.63	Bao et al. (2011)
	chin001	Wulan	37.00	100.00	3600	*Juniperus* sp.	24	1336	1985	650	–	–	Local Met. Bureau & RZ Zu
	chin003	Qilan Mountains	38.17	100.32	3400	*Juniperus* sp.	7	1571	1981	411	–	–	Local Met. Bureau & RZ Zu
	chin004	Huashan	34.48	110.08	2060	*Pinus* sp.	34	1583	1993	411	355.3	0.64	XD Wu
	chin005	Shenge	37.00	98.50	3800	*Juniperus* sp.	243	893	1993	1101	338.5	0.78	Sheppard et al. (2004)
	chin006	Dulan	36.00	98.00	3800	*Juniperus* sp.	132	896	1993	1098	569.4	0.69	Sheppard et al. (2004)
	chin007	Baiyang Valley	43.56	88.09	1815	*Picea* sp.	40	1875	2004	130	109.8	0.85	Cook et al. (2010)
	chin008	Big Kushitai	42.88	82.13	2763	*Picea* sp.	44	1713	2004	292	160.4	0.59	Cook et al. (2010)
	chin009	Jialepake	43.07	82.15	2308	*Picea* sp.	57	1629	2004	376	217.7	0.66	Cook et al. (2010)
	chin010	Kengbulake	42.80	81.72	2593	*Picea* sp.	41	1727	2004	278	213.7	0.62	Cook et al. (2010)
	chin011	Kuerdening	43.15	82.87	1499	*Picea* sp.	46	1688	2004	317	209.6	0.64	Cook et al. (2010)
	chin012	Qiaxi	43.08	82.68	1710	*Picea* sp.	42	1737	2004	268	201.4	0.56	Cook et al. (2010)
	chin013	Shitizi East Valley	43.72	86.72	1865	*Picea* sp.	46	1843	2004	162	129.0	0.70	Cook et al. (2010)
	chin014	Tian Chi	43.88	88.12	1913	*Picea* sp.	49	1722	2004	283	201.2	0.83	Cook et al. (2010)
	chin015	Xiaoxi Valley	43.78	86.30	1878	*Picea* sp.	44	1786	2004	219	149.1	0.70	Cook et al. (2010)
	chin016	Ma'Erkang	31.78	101.92	2500	*Cupressus* sp.	40	1651	2007	357	209.1	0.55	Cook et al. (2010)
	chin017	Xiangchen	28.90	99.75	3980	*Juniperus* sp.	43	1597	2007	411	278.1	0.53	Cook et al. (2010)
	chin018	Daocheng	29.28	100.08	4150	*Abies* sp.	45	1615	2006	392	172.8	0.51	Cook et al. (2010)
	chin019	Xiangcheng Maxiong Valley	29.15	99.93	3530	*Abies* sp.	56	1539	2006	468	282.9	0.80	Cook et al. (2010)
	chin020	Litang	30.23	100.27	4050	*Juniperus* sp.	44	1451	2007	557	331.8	0.48	Cook et al. (2010)
	chin021	Xiangcheng	28.98	99.93	3750	*Abies* sp.	48	1607	2007	401	263.9	0.42	Cook et al. (2010)
	chin022	Xinlong County	30.87	100.28	3300	*Picea* sp.	42	1711	2007	297	201.3	0.72	Cook et al. (2010)
	chin023	Yajiang	30.00	100.87	4020	*Picea* sp.	48	1757	2006	250	162.4	0.56	Cook et al. (2010)
	chin024	Baimang Snow Mountain	28.37	99.03	4260	*Juniperus* sp.	42	1676	2007	332	251.2	0.40	Cook et al. (2010)
	chin025	Pantiange, Weixi County	27.37	99.27	3050	*Abies* sp.	27	1570	2007	438	308.2	0.46	Cook et al. (2010)
	chin026	Shangri La	27.62	99.80	3500	*Abies* sp.	67	1541	2007	467	320.9	0.56	Cook et al. (2010)
	chin027	Pantiange 2, Weixi County	27.33	99.30	3040	*Abies* sp.	41	1460	2007	548	366.1	0.44	Cook et al. (2010)
	chin028	Weixi County	27.33	99.30	3060	*Abies* sp.	43	1628	2007	380	224.1	0.43	Cook et al. (2010)
	chin029	Xinjiaing BLKA	43.85	93.30	2810	*Larix* sp.	91	1702	2002	301	190.5	0.63	Cook et al. (2010)
	chin030	Xinjiaing BLKB	43.83	93.38	2840	*Larix* sp.	51	1746	2002	257	150.3	0.66	Cook et al. (2010)
	chin031	Xinjiaing BLKC	43.82	93.33	2480	*Larix* sp.	59	1811	2002	192	118.7	0.60	Cook et al. (2010)
	chin032	Xinjiaing BLKD	43.82	93.30	2380	*Larix* sp.	44	1816	2002	187	129.8	0.66	Cook et al. (2010)
	chin033	Xinjiaing MIQA	43.77	87.92	1970	*Picea* sp.	52	1712	2002	291	213.9	0.70	Cook et al. (2010)
	chin034	Xinjiaing MIQB	43.80	88.02	2080	*Picea* sp.	60	1685	2002	318	247.6	0.81	Cook et al. (2010)
	chin035	Xinjiaing MULA	43.60	90.22	2250	*Picea* sp.	89	1744	2002	259	188.5	0.65	Cook et al. (2010)
	chin036	Xinjiaing MULB	43.60	90.10	2170	*Picea* sp.	56	1837	2002	166	133.2	0.64	Cook et al. (2010)
	Manggui	Manggui	52.05	122.10	714	*Pinus* sp.	34	1841	2008	168	149.8	0.56	Wang et al. (2011)
	Mengkeshan	Mengkeshan	52.62	124.30	720	*Pinus* sp.	38	1740	2007	268	221.4	0.51	Wang et al. (2011)
	NGNE	Nuogannuoer	47.99	119.38	760–790	*Pinus* sp.	67	1868	2009	142	–	0.68	Bao et al. (2011)
Japan	*japa001*	Kyoto (Yonrinpan)	35.33	135.72	650	*Cryptomeria* sp.	20	1768	1983	216	–	0.50	Kojo, 1987
	japa004	Kyoto (Sanrinpan)	35.32	135.72	760	*Cryptomeria* sp.	20	1905	1983	79	–	0.60	Kojo, 1987
	japa007	Kyoto (Jurinpan)	35.32	135.73	840	*Cryptomeria* sp.	45	1777	1985	209	–	0.59	Kojo, 1987
	japa008	Hokkaido	43.77	142.55	1350	*Picea* sp.	34	1887	1987	101	275.3	0.61	Davi et al. (2001)
	japa009	Kunashir (Kuriles)	43.88	145.60	38	*Quercus* sp.	35	1630	1997	368	292.5	0.61	Cook et al. (2010)
	japa010	Mount Onnebetsu	44.00	145.00	812	*Picea* sp.	52	1603	2000	398	225.3	0.56	Cook et al. (2010)
	japa1	Hiroshima Bay	34.30	132.30	50	*Pinus* sp.	7	1720	2003	284	103.7	0.53	KF Kaiser

Korea	kore001	Peak-Sorak Mountain	38.13	128.47	1500	*Pinus* sp.	93	1693	1998	306	175.9	0.55	Park et al. (2001)
Mongolia	mong001	Hovsgol Nuur	50.76	100.20	2300	*Larix* sp.	13	1785	1993	209	192.1	0.77	Jacoby et al. (1999)
	mong002	Manzshir Hiid	47.76	107.00	1755	*Pinus* sp.	25	1787	1994	208	195.5	0.84	Jacoby et al. (1999)
	mong003	Solongotyn Davaa (Tarvagatay Pass)	48.30	98.93	2420	*Pinus* sp.	90	900	1999	1100	342.8	0.61	Jacoby et al. (1996); D'Arrigo et al. (2001)
	mong004	Terelj	47.90	107.45	1565	*Larix* sp.	43	1820	1994	175	125.9	0.83	Jacoby et al. (1999)
	mong005	Urgun Nars	48.57	110.55	1070	*Pinus* sp.	33	1664	1996	333	214.3	0.83	GC Jacoby
	mong006	Zuun Mod	47.78	107.50	1415	*Larix* sp.	30	1587	1996	410	296.4	0.88	GC Jacoby
	mong007	Turgen-charchira mountai	49.70	91.55	2000	*Larix* sp.	26	1612	1994	383	253.7	0.76	F Schweingruber
	mong008	Horin Bugatyin Davaa	49.37	94.88	2229	*Pinus* sp.	15	1694	1998	305	219.9	0.62	D'Arrigo et al. (2000)
	mong009	Khalzan Khamar	49.92	91.57	2500	*Larix* sp.	38	1407	1998	592	333.7	0.73	D'Arrigo et al. (2000)
	mong010	Suuleen Bagtraa	47.27	100.03	2500	*Larix* sp.	33	1426	1999	574	386.6	0.73	D'Arrigo et al. (2000)
	mong011	Zuun Salaa Mod	48.15	100.28	1900	*Larix* sp.	36	1565	2001	437	337.9	0.81	Davi et al. (2006)
	mong012	Undur Ulaan	48.82	103.23	1400	*Larix* sp.	27	1546	2002	457	312.3	0.80	Davi et al. (2006)
	mong013	Telmen Hovoo	48.77	97.12	1841	*Larix* sp.	28	1645	1998	354	280.0	0.70	Davi et al. (2006)
	mong014	Suulchyin Medee	49.48	100.83	1800	*Larix* sp.	29	1613	2002	390	335.3	0.87	Davi et al. (2006)
	mong015	Khorgo Lava	48.17	99.87	2060	*Larix* sp.	64	1432	2000	569	296.4	0.79	Davi et al. (2006)
	mong016	Ankhny Khoton	48.60	88.37	2100	*Larix* sp.	38	1565	2004	440	315.2	0.63	Cook et al. (2010)
	mong017	Biarum Gergj	49.97	91.00	2125	*Larix* sp.	22	1488	2005	518	424.5	0.69	Cook et al. (2010)
	mong018	Biarum Uul	49.97	90.98	2358	*Larix* sp.	24	1547	2005	459	366.8	0.66	Cook et al. (2010)
	mong020	Dayan Nuur	48.27	88.87	2238	*Larix* sp.	18	1664	2005	342	314.4	0.65	Cook et al. (2010)
	mong021	Hentii Mountains	48.35	107.47	2325	*Larix* sp.	84	1032	2001	970	364.4	0.57	Cook et al. (2010)
	mong022	Inferno Ridge	48.08	111.07	1286	*Pinus* sp.	38	1703	1996	294	179.4	0.81	Cook et al. (2010)
	mong023	Khar Uzuur	49.05	94.58	1481	*Larix* sp.	27	1670	1998	329	264.6	0.84	Cook et al. (2010)
	mong024	Khoton Nuur	48.05	88.05	2253	*Larix* sp.	34	1502	2004	503	342.7	0.68	Cook et al. (2010)
	mong025	Khovd Golgi	48.70	88.80	2046	*Larix* sp.	21	1625	2004	380	307.5	0.66	Cook et al. (2010)
	mong026	Mandal Hill Monastery	46.82	100.12	2309	*Larix* sp.	23	1452	2002	551	294.2	0.71	Cook et al. (2010)
	mong027	ND Bayanhangor	46.32	101.32	2700	*Larix* sp.	21	1609	2001	393	309.3	0.71	Cook et al. (2010)
	mong028	Onon Gol	48.08	111.68	1200	*Larix* sp.	25	1662	2001	340	227.2	0.71	Cook et al. (2010)
	mong029	Ovoont	49.87	91.43	1939	*Larix* sp.	36	1462	1998	537	379.5	0.77	Cook et al. (2010)
	mong030	South Park Ridge	49.38	94.88	2333	*Larix* sp.	45	1465	1998	534	311.4	0.74	Cook et al. (2010)
	mong031	Zuun Mod Gol	48.25	97.40	1942	*Larix* sp.	30	1549	1998	450	356.3	0.64	Cook et al. (2010)
	mong032	Zurkh Togol	46.52	100.95	2566	*Larix* sp.	47	1506	2002	497	287.2	0.60	Cook et al. (2010)
	mong033	Horin Bugatiyn	49.37	94.88	2382	*Larix* sp.	43	1615	1997	383	304.0	0.52	Cook et al. (2010)

Table 1 (*Continued*)

Country	Site code	Site Location	Lat (°N)	Long (°E)	Elev (m a.s.l.)	Genus	Series (N)	Start year (>5 N)	End year	Length (>5 N)	MSL	Rbar	Investigator
Russia	Khotugn	Khotugn	63.38	125.80	100	*Pinus* sp.	28	1687	1991	305	231.2	0.65	Wang et al. (2011)
	russ020	Baikalsee, Irkutsk	53.60	105.00	700	*Pinus* sp.	12	1895	1978	84	81.8	0.59	F Schweingruber
	russ050	Zhigansk	66.52	122.33	180	*Pinus* sp.	31	1717	1991	275	209.9	0.65	F Schweingruber
	russ055	Khotugn-Uladan-Tukulan	63.38	125.80	100	*Pinus* sp.	28	1687	1991	305	257.3	0.65	F Schweingruber
	russ057	Khandiga-River	62.47	137.75	400	*Picea* sp.	24	1772	1991	220	172.8	0.56	F Schweingruber
	russ085	Tschuchonoi-River	61.15	136.57	600	*Picea* sp.	28	1684	1992	309	277.9	0.61	F Schweingruber
	russ103	Sartan River	64.93	132.93	750	*Larix* sp.	32	1652	1991	340	222.5	0.66	F Schweingruber
	russ105	Bryungjade River	63.62	141.35	750	*Larix* sp.	32	1648	1991	344	235.7	0.76	F Schweingruber
	russ108	Baraii River	63.65	133.78	200	*Larix* sp.	17	1731	1992	262	184.5	0.61	F Schweingruber
	russ112	Yakutsk-Biol.Station	62.22	129.35	270	*Larix* sp.	26	1792	1991	200	167.3	0.69	F Schweingruber
	russ129	Ceminsky pass	51.00	85.63	1450	*Larix* sp.	29	1631	1994	364	279.7	0.61	F Schweingruber
	russ130	Jablonsky pass East	50.87	85.23	1450	*Larix* sp.	30	1655	1994	340	250.4	0.72	F Schweingruber
	russ131	Tyn hill	54.23	89.58	650	*Pinus* sp.	30	1653	1994	342	214.3	0.75	F Schweingruber
	russ135	Aktasch Valley	50.42	87.58	2000	*Larix* sp.	30	1613	1994	382	287.4	0.68	F Schweingruber
	russ137	Ust Ulagan Lake	50.48	87.65	2150	*Larix* sp.	24	1636	1994	359	229.0	0.74	F Schweingruber
	russ139	Ust Koksa valley	50.15	85.37	1700	*Picea* sp.	26	1810	1994	185	136.7	0.52	F Schweingruber
	russ140	Kirisky pass	50.65	84.98	1500	*Larix* sp.	30	1742	1994	253	229.3	0.73	F Schweingruber
	russ157	Taksimo dry	56.33	114.67	510	*Pinus* sp.	32	1719	1996	278	218.1	0.64	F Schweingruber
	russ167	Sarma	53.18	106.88	500	*Pinus* sp.	26	1715	1996	282	196.9	0.83	F Schweingruber
	russ169	Kodarpass (Baikal)	56.50	117.25	1000	*Picea* sp.	24	1721	1996	276	235.9	0.70	F Schweingruber
	russ170	Severobaikalsk, dry	55.25	109.50	540	*Pinus* sp.	28	1746	1996	251	182.3	0.81	F Schweingruber
	russ172	Tschita, Dünen Süd	56.83	118.83	700	*Pinus* sp.	28	1756	1996	241	172.5	0.66	F Schweingruber
	russ174	White-River, P.Tung.	61.85	93.40	120	*Picea* sp.	28	1788	1994	207	176.5	0.71	F Schweingruber
	russ175	Nirukda, P.Tung.	61.93	95.15	160	*Picea* sp.	24	1764	1994	231	162.8	0.48	F Schweingruber
	Taksimo	Taksimo	56.33	114.67	510	*Pinus* sp.	32	1719	1996	278	218.1	0.64	Wang et al. (2011)
	Tschita	Tschita	56.83	118.08	700	*Pinus* sp.	28	1756	1996	241	169.0	0.66	Wang et al. (2011)
	Zhigansk	Zhigansk	66.52	122.33	180	*Pinus* sp.	31	1728	1991	264	163.5	0.62	Wang et al. (2011)

Table 2
Climate reconstruction characteristics, including geographical location (latitude and longitude in degrees), used proxies reconstructed variable, total length, start and end year, and investigator (reference).

Location	Proxy	Lat (°N)	Long (°E)	Reconstructed variable	Length	Start year	End year	Investigator
North-Central China (Region A)	TRW, historical documents	33–36°	108–112°	April–July Precip (mm)	401	1600	2000	Yi et al. (2010)
North-Central China (Region B)	TRW, historical documents	38–41°	110–114°	June–August Precip (mm)	401	1600	2000	Yi et al. (2010)
North-Central China	TRW, historical documents	33–41°	108–115°	June–August Precip (Index)	533	1470	2002	Yi et al. (2012)
North-Central China	TRW, historical documents	33–41°	108–115°	June–August Temp (Index)	533	1470	2002	Yi et al. (2012)
Huashan, Shaanxi Province, China	TRW, MXD	34°29'	110°05'	May–June Precip (mm)	389	1600	1988	Hughes et al. (1994)
Huashan, Shaanxi Province, China	TRW	34°29'	110°05'	April–July Precip (mm)	389	1600	1988	Hughes et al. (1994)
Eastern China	Speleothem	39°47'	115°56'	May–August Temp (°C, Index)	2651	–665	1985	Tan et al. (2003)
Eastern Tibet, China	TRW	31°07'	97°02'	Aug–September Temp (°C)	396	1600	1995	Bräuning and Mantwill (2004)
Mongolia, Central Asia	TRW	49°15'	100°40'	April–October Streamflow (m^3/s)	361	1637	1997	Davi et al. (2006)
Northern Japan, northwest Pacific	TRW, MXD	43°35'	142°42'	April–September Temp (°C)	441	1557	1997	Davi et al. (2001)

Methods

The East Asian TRW network contains seven records which were only available as standardized TRW chronologies, and were thus included in this study without any changes. The remaining 99 TRW datasets were initially quality checked using the TSAP program (LINTAB^{TM}-5, RinnTech) for visual agreement, and subsequently with the COFECHA software (Holmes, 1983) for statistical control of the data. Based on this quality control, three datasets were corrected (chin032, mong032, russ055), and one was excluded (mong019). To remove the biological age trend, all raw TRW measurements were detrended with a negative exponential and linear regression curve fit, using the software ARSTAN (Cook and Krusic, 2005). In the subsequent analyses, we used the standardized (STD) site chronologies, where the chronologies were truncated at <5 series.

The spatiotemporal analyses in this study were based on correlation analyses. The significance of the correlations was estimated using two sided *t*-tests. As we were interested in the SNAO-East Asia climate association on both short (interannual) and long (decadal and above) time scales, the correlation analyses were performed both on high- and low-pass filtered time series. A Gaussian M-term

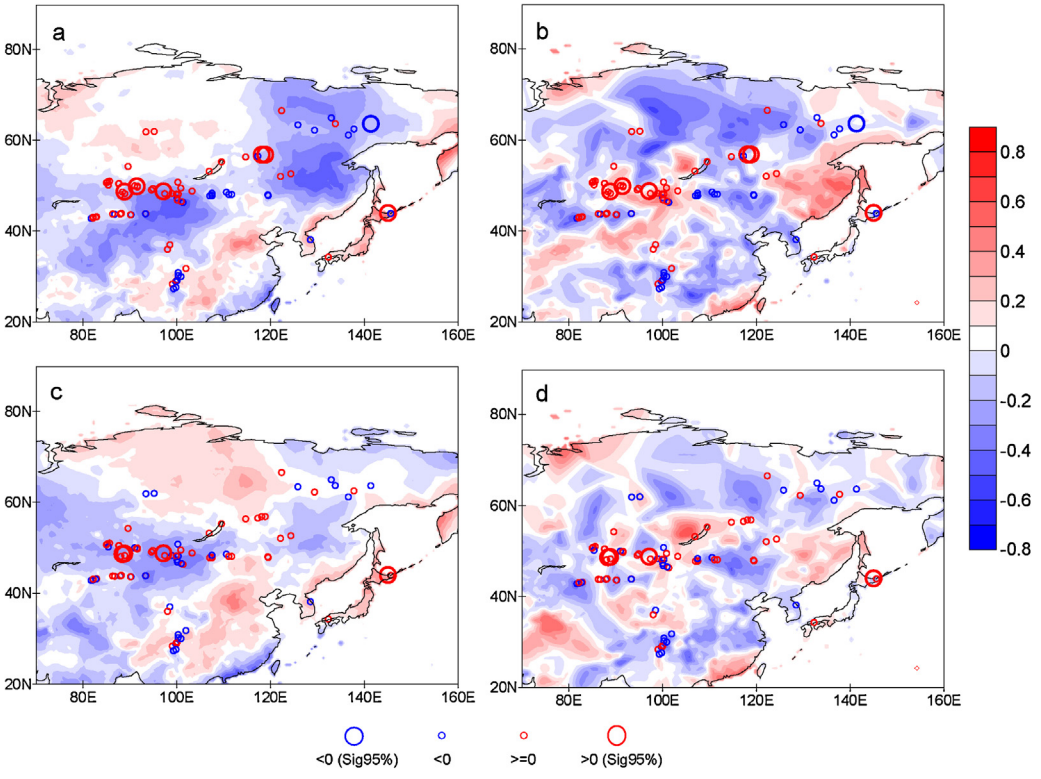

Fig. 3. Correlation between observed (a) and (b) and reconstructed (c) and (d) SNAO and a set of East Asian tree-ring chronologies during 1951–1990. All data was high-pass filtered. To facilitate the interpretation, the spatial correlation patterns between observed SNAO and JA mean temperature (a, c) and total JA precipitation (b, d) from Fig. 1 are also shown as background.

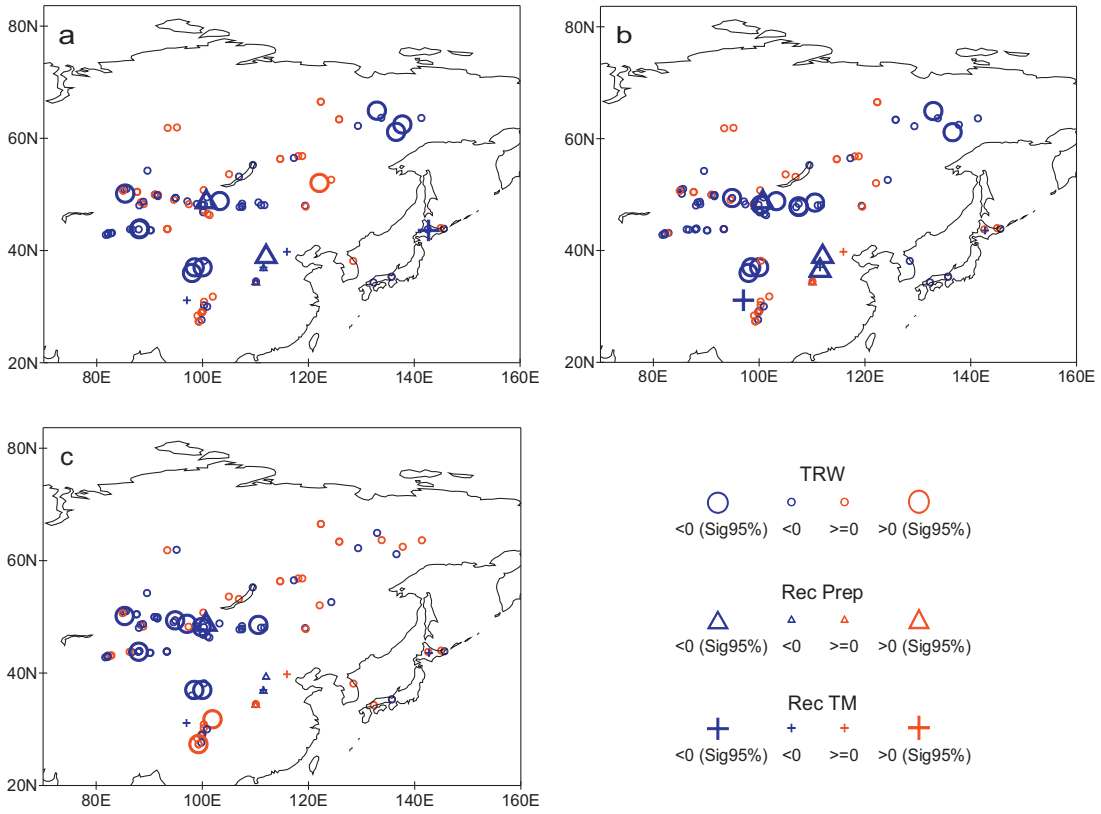

Fig. 4. Correlation during 1901–1978 between the tree-ring width (TRW) data (circles), climate reconstructions (reconstructed precipitation: triangles, reconstructed temperature: cross) and (a) JJA HadSST1 Niño 3 index (Rayner et al., 2003), (b) DJF HadSST1 Niño 3 index and (c) the reconstructed DJF Niño 3 index (Cook, 2000). Note that the proxies were correlated with DJF Niño 3 following the summer season, e.g. JJA TRW in 1901 was correlated against the DJF Niño 3 index of 1901–1902 (see text for further explanation).

high-pass filter was used to remove the long-term variations from the time series, highlighting periods of ≤9 years, and a low-pass filter to represent longer timescales. Moreover, since the variability of both the SNAO and climate in East Asia are influenced by the ENSO (e.g. Chang et al., 2000; Folland et al., 2009), we also utilized partial correlations to explore the relationships between the SNAO and TRW data/reconstructions, which are statistically independent of ENSO, over the last four centuries. For more details on partial correlations, see Linderholm et al. (2011). To get the significance levels of the smoothed time series, a Monte–Carlo experiment was used and the data was high-pass filtered before the experiment, similar to the method introduced by McCabe et al. (2004).

Results

Network characteristics

The East Asian TRW network consisted of 106 chronologies from five countries including 39 sites from China, 32 sites from Mongolia, 27 sites from Russia, 7 from Japan and 1 from Korea (Table 1). The genera distribution of the assemblage, without considering the species, included 40 chronologies of *Larix* sp., 24 of *Pinus* sp., 23 of *Picea* sp., 7 each of *Abies* sp. and *Juniperus* sp., 3 of *Cryptomeria* sp., and 1 of *Cupressus* sp. Only one chronology was constructed from a deciduous species; *Quercus* sp. The minimum sample size of the chronologies was seven series (japa1 and chin003), while the maximum number was 243 series for the Shenge site in China (chin005). After truncation at <5 series, the Kyoto (Sanrinpan) site in Japan provided the shortest TRW chronology with 79 years (1905–1983 AD), and the Shenge site in China the longest with 1101 years (893–1993 AD). Mean segment length (MSL) ranged from 81 to 569 years, with a network average of 243 years. Although no significant errors could be detected, the inter-series correlations of all sites varied rather strongly between 0.40 and 0.88, yielding a network average of 0.66.

Spatiotemporal analysis

To allow a comparison between the results found by Linderholm et al. (2011), Fig. 3a and b shows the spatial correlation between the observed SNAO and TRW data/climate reconstructions records in 1951–1990. In general, positive correlations between SNAO and TRW are found in Mongolia and north-western China, while negative correlations are mainly found in the eastern parts of the region. Most of the few significantly correlated chronologies are found in the regions where strong correlations between the SNAO and observed climate is found; Mongolia, northern Japan and north-eastern Russia. When the reconstructed SNAO data is used (Fig. 3c and d), a similar correlation pattern as above is obtained, although the correlations are weaker, both for observed climate and TRW data/reconstructions. The only significant correlations are found in Mongolia and northern Japan.

The influence of ENSO on the proxy data, as seen from correlation between the TRW chronologies/climate reconstructions and observed and reconstructed Niño 3 records over the common 1901–1978 period, is shown in Fig. 4. First of all, the correlation patterns for observed (Fig. 4a) and reconstructed (Fig. 4b) ENSO were quite similar in terms of positive and negative correlations. The major differences between the two patterns are the slightly stronger correlations in Mongolia and weaker correlations in

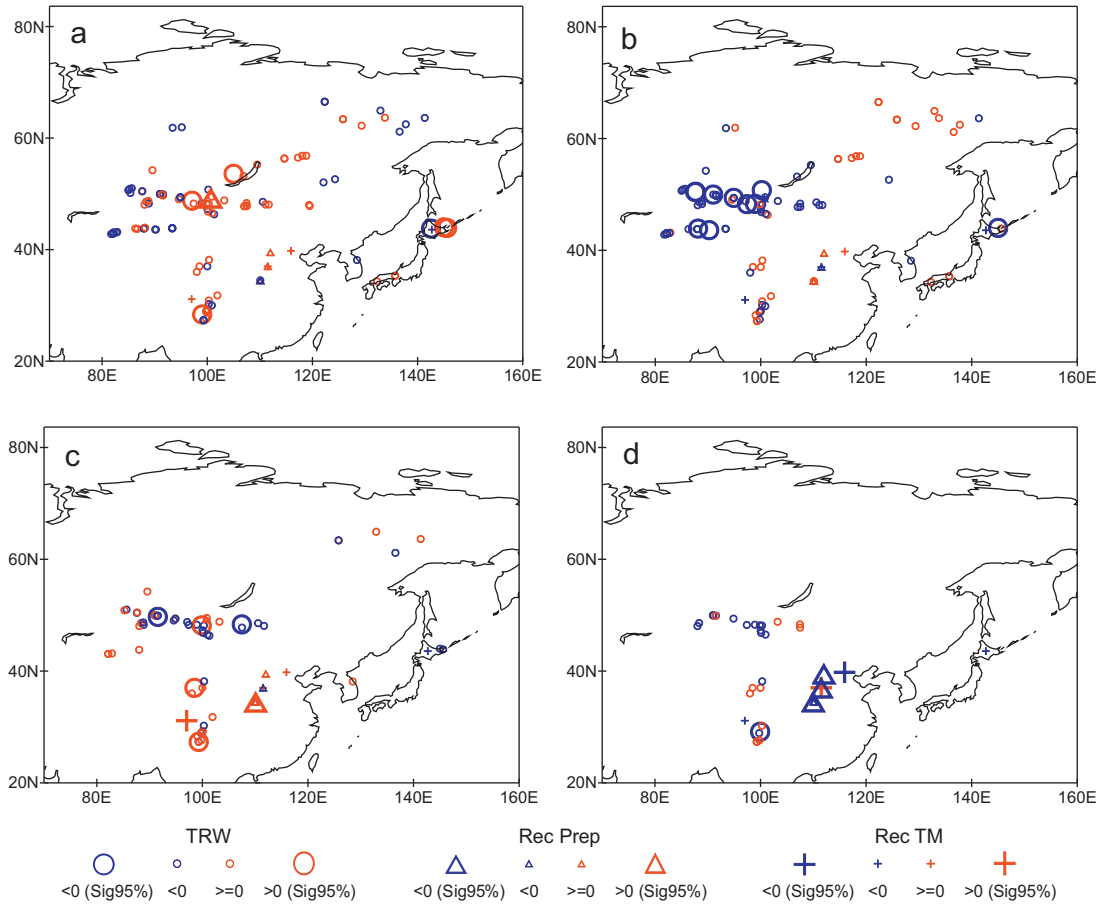

Fig. 5. Partial correlations, independent of the DJF Niño 3 index (Cook, 2000), between high-pass filtered reconstructed SNAO index and tree-ring width data (TRW), reconstructed precipitation (Rec Prep) and temperature (Rec TM) for the (a) 1901–1978, (b) 1801–1900, (c) 1701–1800 and (d) 1601–1700 periods.

central China using the observed compared to the reconstructed ENSO. Based on the coherence in spatial correlation patterns for the two ENSO indices, we assume that the Niño 3 reconstruction is useful for removing the ENSO signal in the TRW data prior to the twentieth century.

Analyzing the temporal associations between the SNAO and East Asian TRW network, correlations for the last four centuries were carried out using 100-year time windows (except during the twentieth century), representing the 1601–1700, 1701–1800, 1801–1900, 1901–1978 periods. Prior to the analyses, all data were high- and low-pass filtered to highlight the variability at high and low frequencies, respectively (Figs. 5 and 6). Results in the high frequency domain point to a rather diffuse response pattern in the twentieth century across the entire region (Fig. 5 a). In general, the signs of the correlations are opposite from those found for reconstructed ENSO (Fig. 4b), and while both indices show significant correlations with sites in southern China, the significant SNAO correlations are found at a slightly higher latitude. The correlation pattern is more coherent in the nineteenth century (Fig. 5b), where almost all TRW sites in and surrounding Mongolia show negative correlations, several significant, with the SNAO. Elsewhere, the significant correlations in southern China are now reduced, and the significant correlation in northern Japan changed sign. Also, there is a tendency for more positive (but not significant) correlations in the north-eastern part of the network. In the eighteenth century (Fig. 5c), the correlation pattern changes again, showing strong positive correlations in central and southern China, and a mixed pattern in the Mongolian region. In the seventeenth century (Fig. 5d), the few sites covering this period show a west-east pattern in the Mongolian region, with (mainly) negative correlations in the west and positive in the east. There are (non-significant) positive correlations in central China, but no coherent pattern in the south.

The low-frequency correlation pattern (Fig. 6) differs from that of the high frequency. In the twentieth century (Fig. 6a), the pattern is heterogeneous, similar to that at the high frequency, but more correlations are significant. There is an indication of a west-east gradient in correlations in the Mongolian region, and significant negative correlations are found along the eastern edge of the Tibetan Plateau. In Eastern China, significant negative correlations are found for the two temperature reconstructions, but positive for the precipitation reconstruction, which is opposite of what was expected from Fig. 1. In the nineteenth century (Fig. 6b), there is a tendency for more negative correlations in the central part of East Asia, and most strong correlations are found in this region. In general, the number of significant correlations has decreased from the twentieth century. The eighteenth century (Fig. 6c) displays strong correlations, predominantly along the 50° latitude, while negative correlations are found at southern latitudes. Correlations in the seventeenth century (Fig. 6d) are few and in general negative and not significant. Significant correlations are found along the eastern Tibetan plateau (negative) and at one site in the Mongolian region (positive).

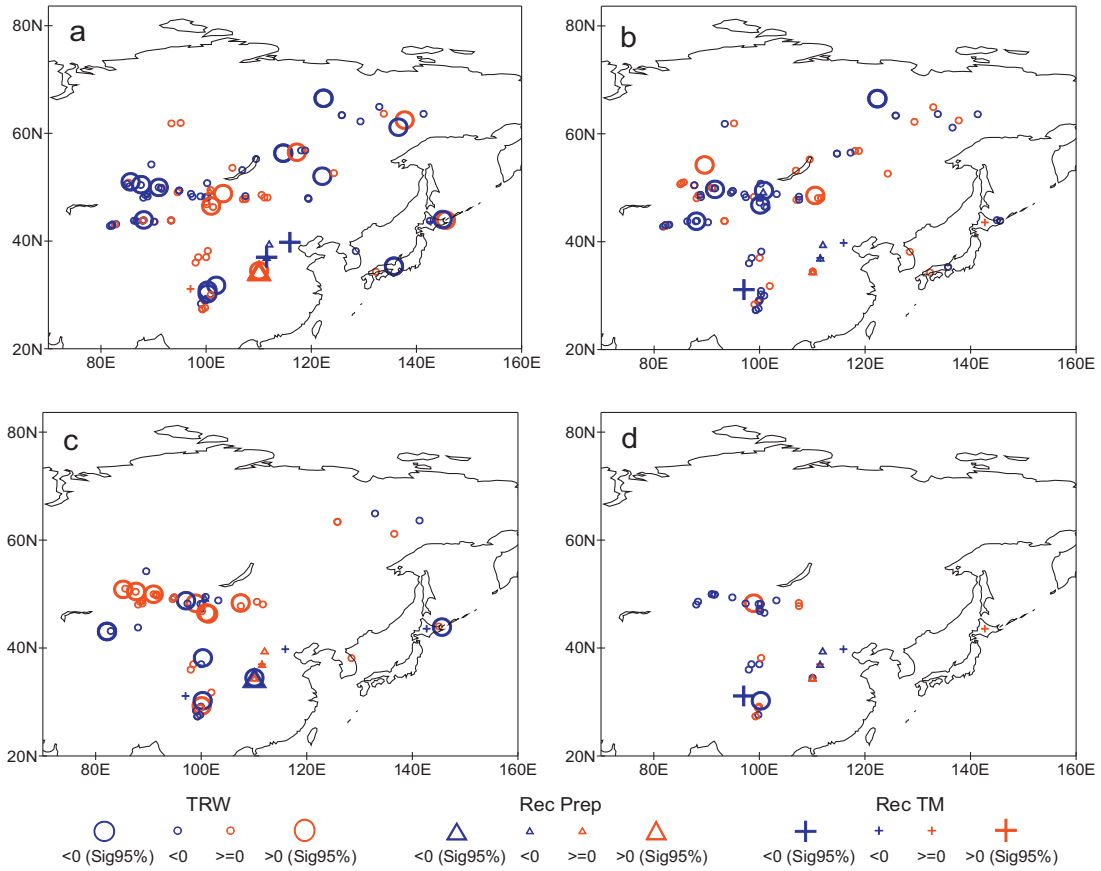

Fig. 6. Same as in Fig. 6, but on decadal timescales (9 point low-pass filtered data): (a) 1901–1978, (b) 1801–1900, (c) 1701–1800, and (d) 1601–1700. The confidence intervals for the correlation coefficients were calculated with a Monte-Carlo experiment.

The temporal stability of the correlation patterns

From Fig. 7, it is clear that there is a large temporal variability in the correlations between the SNAO and the East Asian network throughout the last 400 years. Moreover, the results also show that the influence of ENSO is highly variable as well. When the high-frequency is concerned, there is no coherency in the relative influence of SNAO and ENSO on the TRW chronologies. As expected, the temporal influence of ENSO is quite limited in Mongolia (Fig. 7a–c), but it is seemingly low also in Japan (Fig. 7f). In the sites outside Mongolia (Fig. 7d–i), there is an indication of opposite influences of SNAO and ENSO. Looking at the longer timescales, the running correlation patterns of SNAO and ENSO seem to agree better. In general, the ENSO correlation pattern show little long-term variability, and is centred around zero, while there is more variability in the SNAO correlation pattern.

Discussion

One of the aims of this investigation was to assess if TRW data could be used to extend the analysis of the teleconnection between the SNAO and climate in East Asia presented in Linderholm et al. (2011). The results from this rather preliminary study indicate that tree rings do indeed provide possibilities for such long-term studies. It is evident that not all TRW chronologies are suitable for such analyses, but that was not expected. We used, indiscriminately, all the available TRW data from this region, and in doing so it is unavoidable that some data will not contain the sought for climate signal. In fact, previous studies of individual sites or clusters within the network have shown that some chronologies contain climatic information outside the July–August target season (e.g. Hughes et al., 1994: May–June, April–July; Bao et al., 2011: April–September), and that would have an effect of the correlations. Moreover, the studied area encompasses a large range of climatic zones, from subtropical to subarctic, and from continental to maritime, and there is also a huge span in elevation among the sites (the altitude difference was 4210 m from the lowest to the highest sampled site in the network). Most of the included TRW chronologies would have been developed with a focus on local climate variability, being sampled at sites where a strong temperature or precipitation/drought signal would have been expected. This dependency on local site conditions could explain the sometimes seemingly contradictory correlations for TRW chronologies located close to each other. This would be especially evident when the altitude is concerned. As an example, D'Arrigo et al. (2001) found that trees at the timberline (2420 m a.s.l.) in Mongolia contain a distinct temperature signal, whereas Davi et al. (2006) successfully developed a stream flow (drought) reconstruction for mid- to high-altitudes sites (1400–2060 m a.s.l.) in the Selenge river basin, west-central Mongolia.

It should also be noted that in Linderholm et al. (2011), the SNAO-East Asian climate link was mainly attributed to the change in the storm track and propagation of quasi-stationary waves associated with the SNAO phase, which is prevailing on intra-seasonal timescales. This may explain why the SNAO signal is not so efficiently recorded at some sites, particularly in the high (interannual)

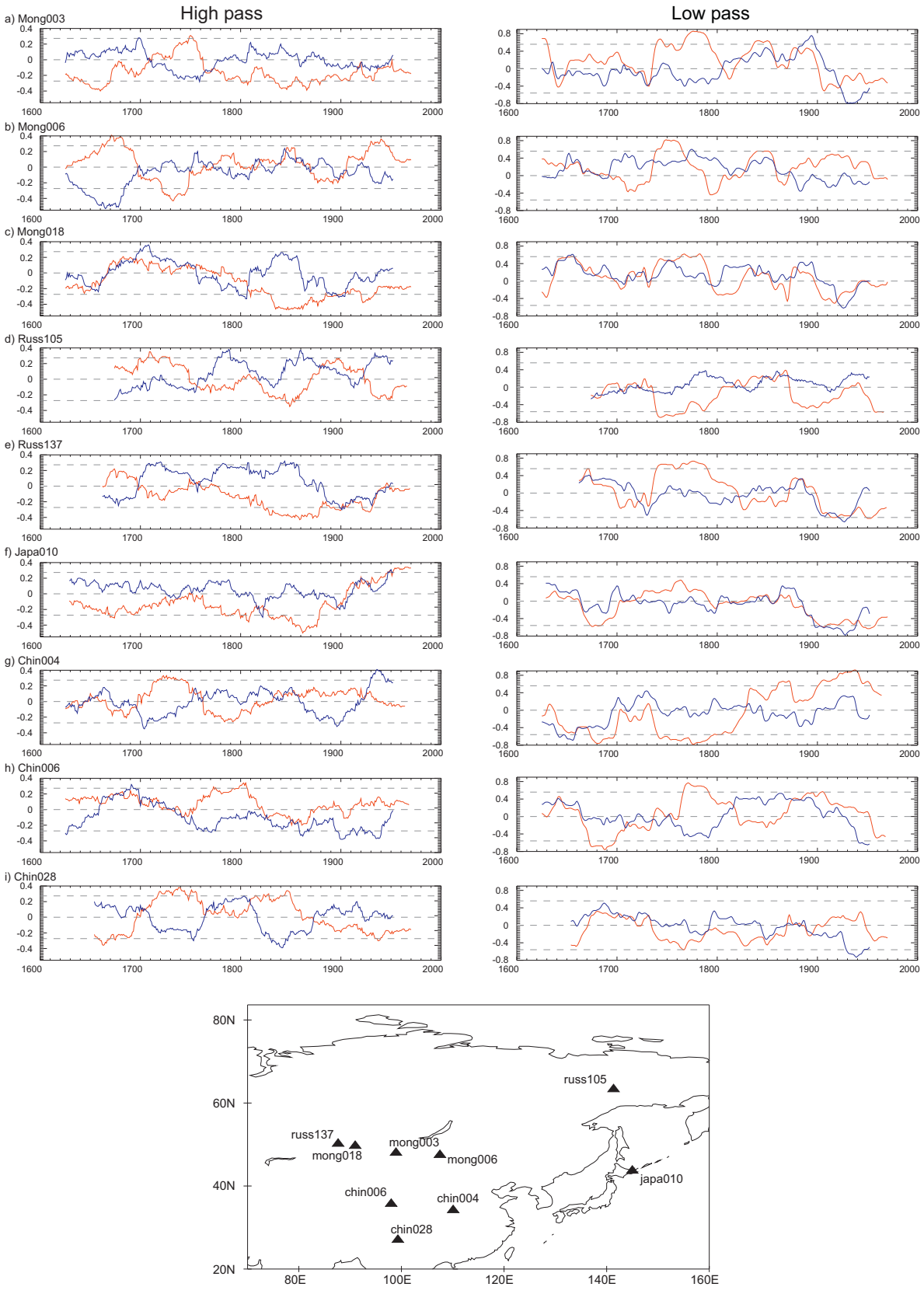

Fig. 7. 51-year running correlations between the SNAO (red line) and reconstructed DJF Niño 3 index (blue line) and tree-ring width chronologies from 9 selected sites (a)–(i). Left panel shows running correlations with high-pass filtered data, and the right panel low-pass filtered data. The significance levels for the low-pass filtered correlations were estimated with a Monte Carlo experiment. The location of the sites is shown in the lower panel.

frequencies. Moreover, as shown in Fig. 5, ENSO periodically shows a much stronger relationship with East Asian TRW data than the SNAO. This is of course expected due to the significant influence of ENSO on East Asian climate (Wang et al., 2000). It has previously been shown that also the Pacific Decadal Oscillation (PDO, Mantua et al., 1997), described as a long-lived El Niño-like pattern of Pacific climate variability (Mantua and Hare, 2002), influences climate in this region. The correlation between JJA PDO and Niño 3 indices is quite strong (0.48, $p < 0.01$, 1901–2000), and the correlation patterns between the PDO and TRW, and those between the SNAO and TRW with PDO removed, are highly similar to those obtained with Niño 3 (not shown).

Still, the study indicated some regions where the association with the SNAO seems to be particularly strong, especially in the Mongolian region (including some south-central Russian and northwestern Chinese sites), central and western China, where the western China sites are represented by sites on the eastern edge of the Tibetan Plateau, and northern Japan. From Fig. 3, these fall into regions where there are moderately strong correlations between temperature/precipitation and the SNAO. Clearly the TRW chronologies from these regions are constructed from trees that grow close to their limit of distribution, e.g. due to water availability (e.g. the arid parts of central East Asia) or the high elevation (e.g. Tibetan Plateau). These strong associations are not surprising. The geographical location of the Mongolian region makes it influenced by both the East Asian monsoon and westerlies modulated by the NAO (An et al., 2008), while climate variability over the Tibetan Plateau in the late twentieth century has been linked with the NAO, but mainly the winter circulation (e.g. Yu and Zhou, 2004; Xin et al., 2010). Most studies do rely on instrumental data from the latter half of the twentieth century. To give some examples, in Mongolia, Wang H. (2006b) noted an association between May–July precipitation in north-eastern Mongolia and SLP in the SNAO southern node region (see Fig. 2b in Wang H., 2006b), while Li et al. (2009) found a link between the SNAO and runoff in the Aksu River in Xinjiang, northwestern China, on short and long timescales. Liu and Yin (2001) suggested that summer precipitation over the Eastern Tibetan Plateau (ETP) is closely associated with the NAO, where the northern and southern part of the ETP responds differently to NAO variability. This could partly explain the difference in correlation signs of the ETP TRW chronologies in this study. Thus, a more detailed study of the influence of the SNAO should perhaps focus on increasing the chronology density from these particular regions.

From Fig. 7, it may be deduced that the North Atlantic-East Asian teleconnection is not stable through time. Moreover, no coherent pattern among the sites could be found. However, that the teleconnection would be stable was not expected. As shown in Linderholm et al. (2011), the SNAO-East Asian summer climate link is most prominent during very negative or positive SNAO years, and additionally, that analysis was done in a period (1951–2002) when the SNAO was in a predominantly positive phase, possibly anomalous in the last four centuries. Moreover, temporally unstable associations between the NAO and climate in East Asia has previously been shown in instrumental data (Wang et al., 2003; Sun et al., 2008), as well as in proxy data (Lee and Zhang, 2011), and a periodical weakening in the correlation between the SNAO and climate over UK (the southern node) in the 1920s was noted by Greatbatch and Rong (2006, see Fig. 9). The reason for these variable SNAO-East Asia links is yet not understood, but may possibly be associated with changes in the position of the subtropical Jet stream, which is linked with surface climate in East Asia (Liao et al., 2004). Shifts in the position of the jet stream may, in turn, be related to large-scale shifts in the atmospheric or ocean circulation, e.g. the long-term variability of the PDO, or the phases of the Atlantic Multidecadal Oscillation (AMO), which influence the SNAO (Goswami et al., 2006; Folland et al., 2009). A denser TRW network, with focus on chronologies with known strong climate information, possibly selected from a number of key sites (e.g. Tibetan Plateau and the Mongolian region) could provide unique opportunities to make a detailed study of the relative influence of climate features, as well as changes in the large-scale circulation associated with these.

Conclusion

Utilizing an East Asian TRW network, and some additional climate reconstructions, we made a preliminary investigation of the nature of a previously proposed teleconnection between the summer NAO (SNAO) and climate in East Asia. Our results suggest that 1) TRW data from the region are useful to extend the analyses beyond the instrumental period (i.e. pre 1950). Naturally there are some caveats, such as limitation in the spatial coverage of the TRW network as well as the strength of the climate signal in the proxy data. The regions with the strongest SNAO-TRW correlations were found in the central parts of East Asia (in and around Mongolia) and on the eastern edge of the Tibetan Plateau, regions where tress are expected to contain strong climatic signals. 2) The association between the SNAO and East Asian climate, as inferred by the TRW data, over the last 400 years has been highly variable, among regions as well as at single sites. This information may eventually be useful for better understanding the relative importance of different forcings (e.g. NAO and ENSO) on climate, e.g. the East Asian Monsoon, in this part of the world. 3) There was a clear difference in the SNAO-TRW associations between the two examined time scales, being stronger on the decadal and above timescales. This suggests that TRW data can be very useful to explore the SNAO-East Asia teleconnection, and what is driving it, on longer timescales. Moreover, long instrumental records for the last several centuries in East Asia (e.g. Jung et al., 2001), will be utilized in further studies.

Acknowledgements

This work was partly supported by Swedish International Development Cooperation Agency SIDA (project SWE-2009-245). Chris Folland was supported by the Joint DECC/Defra Met Office Hadley Centre Climate Programme (GA01101). Jee-Hoon Jeong was supported by Basic Science Research Program through the National Research Foundation of Korea(NRF) funded by the Ministry of Education, Science and Technology (2012M1A2A2671852). The paper contributes to the CLIVAR International Climate of the Twentieth Century project (http://www.iges.org/c20c/) and the Swedish strategic research areas Modelling the Regional and Global Earth system (MERGE), and Biodiversity and Ecosystem services in a Changing Climate (BECC). Comments from the guest editor and two anonymous reviewers helped to improve the manuscript. This is contribution no. 12 from the Sino-Swedish Centre for Tree-Ring Research (SISTRR). Finally, we express our gratitude to all authors that have provided data through the International Tree-Ring Data Bank.

References

An, C.-B., Chen, F.-H., Barton, L., 2008. Holocene environmental changes in Mongolia: a review. Global and Planetary Change 63, 283–289.

An, Z., 2000. The history and variability of the East Asian paleomonsoon climate. Quaternary Science Reviews 19, 171–187.

Ansell, T.J., et al., 2006. Daily mean sea level pressure reconstructions for the European-North Atlantic region for the period 1850–2003. Journal of Climate 19, 2717–2742.

Bao, G., Liu, Y., Linderholm, H.W., 2011. April-September mean maximum temperature inferred from Hailar pine (*Pinus sylvestris var mongolica*) tree rings in the Hulunbuir region, Inner Mongolia, back to 1868 AD. Palaeogeography Palaeoclimatology Palaeoecology, http://dx.doi.org/10.1016/j.palaeo.2011.10.017.

Barnston, A.G., Livezey, R.E., 1987. Classification, seasonality and persistence of low-frequency atmospheric circulation patterns. Monthly Weather Review 115, 1083–1126.

Bräuning, A., Mantwill, B., 2004. Summer temperature and summer monsoon history on the Tibetan plateau during the last 400 years recorded by tree rings. Geophysical Research Letters 31, L24205.

Chang, C.P., Zhang, Y.S., Li, T., 2000. Interannual and interdecadal variations of the East Asian summer monsoon and tropical Pacific SSTs. Part I: Roles of the subtropical ridge. Journal of Climate 13, 4310–4325.

Cook, E.R., 2000. Nino 3 index reconstruction. International Tree-Ring Data Bank. IGBP PAGES/World Data Center-A for Paleoclimatology, Data Contribution Series #2000-052. NOAA/NGDC Paleoclimatology Program, Boulder, CO, USA.

Cook, E.R., Krusic, P.J., 2005. Program ARSTAN: A Tree-Ring Standardization Program Based on Detrending and Autoregressive Time Series Modelling with Interactive Graphics. Tree-Ring Laboratory, Lamont-Doherty Earth Observatory of Columbia University, Palisades, New York.

Cook, E.R., Anchukaitis, K.J., Buckley, B.M., D'Arrigo, R.D., Jacoby, G.C., Wright, W.E., 2010. Asian Monsoon failure and megadrought during the last millennium. Science 328, 486–489.

D'Arrigo, R., Jacoby, G., Pederson, N., Frank, D., Buckley, B., Nachin, B., Mijiddorj, R., Dugarjav, C., 2000. Mongolian tree rings, temperature sensitivity and reconstructions of Northern Hemisphere Temperature. The Holocene 10, 669–672.

D'Arrigo, R., Jacoby, G., Frank, D., Pederson, N., Cook, E., Buckley, B., Nachin, B., Mijiddorj, R., Dugarjav, C., 2001. 1738 years of Mongolian temperature variability inferred from a tree-ring width chronology of Siberian pine. Geophysical Research Letters 28, 543–546.

D'Arrigo, R., Cook, E., Wilson, R., Allan, R., Mann, M., 2005. On the variability of ENSO over the past six centuries. Geophysical Research Letters 32, L03711.

Davi, N., D'Arrigo, R., Jacoby, G.C., Buckley, B., Kobayashi, O., 2001. Warm-season annual to decadal temperature variability for Hokkaido, Japan, inferred from maximum latewood density (AD 1557-1990) and ring width data (AD 1532-1990). Climatic Change 52, 201–217.

Davi, N.K., Jacoby, G.C., Curtis, A.E., Baatarbileg, N., 2006. Extension of drought records for central Asia using tree-rings: west central. Journal of Climate 19, 288–299.

Ding, Y., 2004. Seasonal March of the East-Asian Summer Monsoon. In: Chang, C.-P. (Ed.), East Asian Monsoon, World Scientific Series on meteorology of East Asia, 2; pp. 3–53.

Folland, C.K., Knight, J., Linderholm, H.W., Fereday, D., Ineson, S., Hurrell, J.W., 2009. The summer North Atlantic Oscillation: past, present, and future. Journal of Climate 22, 1082–1103.

Gong, D., Ho, C. -H., 2003. Arctic oscillation signals in the East Asian summer monsoon. Journal of Geophysical Research 108, 4066.

Goswami, B.N., Madhusoodanan, M.S., Neema, C.P., Sengupta, D., 2006. A physical mechanism for North Atlantic SST influence on the Indian summer monsoon. Geophysical Research Latters 33, L02706.

Greatbatch, R.J., Rong, P.P., 2006. Discrepancies between different northern hemisphere summer atmospheric data products. Journal of Climate 19, 1261–1273.

Gu, W., Li, C., Li, W., Zhou, W., Chan, J.C.L., 2009. Interdecadal unstationary relationship between NAO and east China's summer precipitation patterns. Geophysical Research Letters 36, L13702.

Holmes, R.L., 1983. Computer-assisted quality control in tree-ring dating and measurement. Tree-Ring Bulletin 43, 69–78.

Hong, C.-C., Hsu, H.-H., Chia, H.-H., Wu, C.-Y., 2008. Decadal relationship between the North Atlantic Oscillation and cold surge frequency in Taiwan. Geophysical Research Letters 35, L24707.

Hughes, M.K., Wu, X.D., Shao, X.M., Garfin, G.M., 1994. A preliminary reconstruction of rainfall in north-central China since A.D. 1600 from tree-ring density and width. Quaternary Research 42, 88–99.

Hurrell, J.W., van Loon, H., 1997. Decadal variations in climate associated with the North Atlantic Oscillation. Climatic Change 36, 301–326.

Hurrell, J.W., Folland, C.K., 2002. The relationship between tropical Atlantic rainfall and the summer circulation over the North Atlantic. CLIVAR Exchanges 25, 52–54.

Hurrell, J.W., Kushnir, Y., Ottersen, G., Visbeck, M., 2003. An overview of the North Atlantic Oscillation. AGU Geophysical Monograph 134, 1–35.

Jacoby, G.C., D'Arrigo, D., Davaajamts, T., 1996. Mongolian tree rings and 20th-century warming. Science 273, 771–773.

Jacoby, G., D'Arrigo, R., Pederson, N., Buckley, B., Dugarjav, C., Mijiddorj, R., 1999. Temperature and precipitation in Mongolia based on dendroclimatic investigations. IAWA Journal 20, 339–350.

Jung, H.-S, Lim, G.H., Oh, J.H., 2001. Interpretation of the transient variation in the time series of precipitation amounts in Seoul, Korea. Journal of Climate 14, 2989–3004.

Kojo, Y., 1987. A dendrochronological study of *Cryptmeria japonica* in Japan. Tree-Ring Bulletin 47, 1–21.

Lee, H.F., Zhang, D.D., 2011. Relationship between NAO and drought disasters in northwestern China in the last millennium. Journal of Arid Environments 75, 1114–1120.

Li, H., Jiang, Z., Yang, Q., 2009. Association of North Atlantic Oscillations with Aksu River runoff in China. Journal of Geographical Sciences 19, 12–24.

Li, J., Yu, R., Zhou, T., 2008. Teleconnection between NAO and climate downstream of the Tibetan Plateau. Journal of Climate 21, 4680–4690.

Liao, Q., Gao, S., Wang, H., Tao, S., 2004. Anomalies of the extratropical westerly Jet in the north hemisphere and their impacts on east Asian summer monsoon climate anomalies. Chinese Journal of Geophysics 47, 10–18 (in Chinese with English abstract).

Linderholm, H.W., Folland, C.K., Hurrell, J.W., 2008. Reconstructing summer North Atlantic Oscillation (SNAO) variability over the last five centuries. Tree rings in archaeology, climatology and ecology. TRACE 6, 8–16.

Linderholm, H.W., Folland, C.K., Walther, A., 2009. A multicentury perspective on the summer North Atlantic Oscillation (SNAO) and drought in the eastern Atlantic Region. Journal of Quaternary Science 24, 415–425.

Linderholm, H.W., Ou, T., Jeong, J.-H., Folland, C.K., Gong, D., Liu, H., Liu, Y., Chen, D., 2011. Interannual teleconnections between the summer North Atlantic Oscillation and the summer East Asian Monsoon. Journal of Geophysical Research 116, D13107.

Liu, X.D., Yin, Z.Y., 2001. Spatial and temporal variation of summer precipitation over the eastern Tibetan Plateau and the North Atlantic Oscillation. Journal of Climate 14, 2896–2909.

Mantua, N.J., Hare, S.R., Zhang, Y., Wallace, J.M., Francis, R.C., 1997. A Pacific interdecadal climate oscillation with impacts on salmon production. Bulletin of the American Meteorological Society 78, 1069–1079.

Mantua, N.J., Hare, S.R., 2002. The Pacific Decadal Oscillation. Journal of Oceanography 58, 35–44.

McCabe, G.J., Palecki, M.A., Betancourt, J.L., 2004. Pacific and Atlantic Ocean influences on multidecadal drought frequency in the United States. Proceedings of the National Academy of Sciences 101, 4136–4141.

Mitchell, T.D., Jones, P.D., 2005. An improved method of constructing a database of monthly climate observations and associated high-resolution grids. International Journal of Climatology 25, 693–712.

Park, W.-K., Seo, J.-W., Kim, Y., Oh, J.-H., 2001. July-August temperature of central Korea since 1700 AD: reconstruction from tree-rings of Korean pine (*Pinus koraiensis*). Palaeobotanist 50, 107–111.

Rayner, N.A., Parker, D.E., Horton, E.B., Folland, C.K., Alexander, L.V., Rowell, D.P., Kent, E.C., Kaplan, A., 2003. Global analyses of sea surface temperature, sea ice, and night marine air temperature since the late nineteenth century. Journal of Geophysical Research 108, 4407.

Sheppard, P.R., Tarasov, P.E., Graumlich, L.J., Heussner, K.-U., Wagner, M., Österle, H., Thompson, L.G., 2004. Annual precipitation since 515 BC reconstructed from living and fossil juniper growth of northeastern Qinghai Province, China. Climate Dynamics 23, 869–881.

Sun, J., Wang, H., Yuan, W., 2008. Decadal variations of the relationship between the summer North Atlantic Oscillation and middle East Asian air temperature. Journal of Geophysical Research 113, D15107.

Sung, M.-K., Kwon, W.-T., Baek, H.-J., Boo, K.-O., Lim, G.-H., Kug, J.-S., 2006. A possible impact of the North Atlantic Oscillation on the east Asian summer monsoon precipitation. Geophysical Research Letters 33, L21713.

Sung, M.-K., Lim, G.-H., Kug, J.-S., 2010. Phase asymmetric downstream development of the North Atlantic Oscillation and its impact on the East Asian winter monsoon. Journal of Geophysical Research 115, D09105.

Tan, M., Liu, T.S., Hou, J., Qin, X., Zhang, H., Li, T., 2003. Cyclic rapid warming on centennial-scale revealed by a 2650-year stalagmite record of warm season temperature. Geophysical Research Letters 30, 1617.

Trenberth, K.E., 1997. The definition of El Niño. Bulletin of the American Meteorological Society 78, 2771–2777.

Visbeck, M.H., Hurrell, J.W., Polvani, L., Cullen, H.M., 2001. The North Atlantic Oscillation: past, present and future. Proceedings of the National Academy of Sciences of the United States of America 98, 12877–12879.

Wang, B., Wu, R., Fu, X., 2000. Pacific-East Asian Teleconnection: How Does ENSO Affect East Asian Climate? Journal of Climate 13, 1517–1536.

Wang, B., 2006a. The Asian Monsoon. Springer/Praxis Publishing Co, New York, 787 p.

Wang, H., 2006b. Linkage between the northeast Mongolian precipitation and the Northern hemisphere zonal circulation. Advances in Atmospheric Sciences 23, 659–664.

Wang, N., Thompson, L.G., Davis, M.E., Mosley-Thompson, E., Yao, T., Pu, J., 2003. Influence of variations in NAO and SO on air temperature over the northern Tibetan Plateau as recorded by δ18O in the Malan ice core. Geophysical Research Letters 30, 2167.

Wang, X., Brown, P.M., Zhang, Y., Song, L., 2011. Imprint of the Atlantic Multidecadal Oscillation on tree-ring widths in Northeastern Asia since 1568. PLoS ONE 6, e22740.

Wen, X.Y., Wang, S.W., Zhu, J.H., Viner, D., 2006. An overview of China climate change over the 20th century using UK UEA/CRU high resolution grid data. Chinese Journal of Atmospheric Sciences 30, 896–904 (in Chinese with English abstract).

Xin, X., Yu, R., Zhou, T., Wang, B., 2006. Drought in late spring of south China in recent decades. Journal of Climate 19, 3197–3206.

Xin, X.G., Zhou, T.J., Yu, R.C., 2010. Increased Tibetan Plateau snow depth: an indicator of the connection between enhanced winter NAO and late-spring tropospheric cooling over East Asia. Advances in Atmospheric Sciences 27, 788–794.

Yi, L., Yu, H., Xu, X., Yao, J., Su, Q., Ge, J., 2010. Exploratory precipitation in North-Central China during the past four centuries. Acta Geologica Sinica 84, 223–229.
Yi, L., Yu, H., Ge, J., Lai, Z., Xu, X., Qin, L., Peng, S., 2012. Reconstructions of annual summer precipitation and temperature in north-central China since 1470 AD based on drought/flood index and tree-ring records. Climatic Change 110, 469–498.
Yu, R.C., Zhou, T.J., 2004. Impacts of winter-NAO on March cooling trends over subtropical Eurasia continent in the recent half century. Geophysical Research Letters 31, L12204.